Mol Biol Rep (2014) 41:2217–2228
DOI 10.1007/s11033-014-3073-1

Rapamycin inhibition of CFA-induced lymphangiogenesis in PLN is independent of mast cells

Rui-Cheng Ji · Yuki Eshita

Received: 5 February 2013 / Accepted: 4 January 2014 / Published online: 14 January 2014
© Springer Science+Business Media Dordrecht 2014

Abstract Elucidation of the events responsible for the interaction between lymphatic endothelial cells (LECs) and mast cells (MCs) may prove to be a valuable source for controlling lymphangiogenesis. In the present study, we compared immunohistochemical and RT-PCR findings of the popliteal lymph node (PLN) and footpad skin in C57BL/6J and WBB6F1 mice, the MC-deficient strain. The results indicated that MCs play certain role in complete Freund's adjuvant-induced intranodal lymphangiogenesis. VEGF-A, VEGFR-2 and TNF-α were crucial factors in lymphangiogenesis both in the PLN and skin. Moreover, the in vivo administration of the specific mTOR inhibitor, rapamycin inhibited lymphangiogenesis independent of MCs in PLN rather than in the skin. Further study on anti-lymphangiogenic effect will contribute to our understanding of LEC and MC modulation in pathological lymphangiogenesis.

Keywords Lymphangiogenesis · Mast cells · Complete Freund's adjuvant · Rapamycin · VEGF-A · TNF-α

R.-C. Ji (✉)
Department of Human Anatomy, Faculty of Medicine, Oita University, Oita 879-5593, Japan
e-mail: ji@oita-u.ac.jp

Y. Eshita
Department of Infectious Disease Control, Faculty of Medicine, Oita University, Oita, Japan

Introduction

Lymphangiogenesis in tissue inflammation and tumor cell dissemination depends on a complex interplay of interstitial cells, growth factors and extracellular matrix [1, 2]. Recently, the role of mast cells (MCs) involved in immune responses has been attracting attention in terms of their participation in tumor neovascularization. MCs release a wide variety of mediators upon activation including chemokines and cytokines, e.g., TNF (tumor necrosis factor)-α, into extracellular environment [3]. Human MCs express vascular endothelial growth factor (VEGF)-A, VEGF-C and VEGF-D at both the mRNA and protein level [4]. Particularly, the possibility of VEGF-C as a potential therapeutic target has been deeply studied in the last decade. Blocking VEGF-C for controlling lymphangiogenesis has provided an important tool for treatment and prevention of lymphedema, and for inhibition of tumor metastasis. The mammalian target of rapamycin (mTOR) with immunosuppressant and antiproliferative properties is a downstream signal in the VEGF-C/D pathway. The specific mTOR inhibitor rapamycin has been suggested to suppress lymphangiogenesis in animal tumor models [5–7]. However, it still remains to be known whether MCs are involved in inflammation-induced lymphangiogenesis, and whether rapamycin administration affects the interplay between MCs and lymphatic endothelial cells (LECs).

In the present study, we compared complete Freund's adjuvant (CFA)-induced lymphangiogenesis in the skin and lymph nodes of C57BL/6J and WBB6F1 mice. A possible relation of mutual dependence between MCs and LECs was emphasized by studying tissue lymphangiogenesis in WBB6F1 mice, the MC-deficient strain. Hence, rapamycin administration in two strains of mice will contribute to further assess the impact of mTOR inhibition and the role of MCs on lymphangiogenesis.

Materials and methods

Animal models

Female C57BL/6J and the MC-deficient WBB6F1-W/W^v (mutant stock, spontaneous mutation) mice at 8 weeks old were purchased from Japan SLC, Inc. (Shizuoka, Japan). All experiments with mice were performed according to protocols approved by the Animal Research Ethics Committee of Oita University Faculty of Medicine. Mice were injected subcutaneously in the hind footpads with 20–25 μl of an emulsion containing equal volumes of CFA/keyhole limpet hemocyanin in sterile PBS (2.5 mg/ml) (Sigma-Aldrich, St. Louis, MO; Thermo Scientific, Rockford, IL, USA). To assess the possible involvement of MCs in lymphangiogenesis, both the inflammatory footpads and draining popliteal lymph nodes (PLN) were removed at 2, 4, 7 days and 2, 4 weeks ($n = 3$ for each group), and examined using immunohistochemical and reverse transcription polymerase chain reaction (RT-PCR) techniques. PLN weight was also measured after dissecting attached adipose tissue.

Rapamycin treatment

Rapamycin (Wako Pure Chemical Industries, Ltd., Osaka, Japan) was dissolved in methanol at a stock concentration of 25 mg/ml, and diluted in freshly prepared solution (4 % ethanol, 5 % polyethylene glycol 400, and 5 % Tween 80) before use. Both WBB6F1 and C57BL/6J mice were injected intraperitoneally with rapamycin (1 mg/kg) for 2 or 4 weeks every second day immediately after CFA administration ($n = 3$ for each group).

Immunohistochemistry

Paraffin sections of the footpad skin or PLN fixed with 10 % neutral formalin in 0.1 M PBS (pH 7.4) were soaked in 0.3 % hydrogen peroxide and 10 % blocking serum. Sections were incubated with antibodies to podoplanin (hamster anti-mouse IgG, 1:200; AngioBio Co., Del Mar, CA, USA), LYVE-1 (rabbit anti-mouse IgG, 1:100; RELIATech GmbH, Braunschweig, Germany), von Willebrand factor (vWF; rabbit anti-human vWF IgG, 1:300; Dako, Glostrup, Denmark) for 60 min at room temperature or overnight at 4 °C. The subsequent incubation in biotinylated goat anti-rabbit IgG or goat anti-hamster IgG diluted to 1:100–200 was followed by treatment with streptavidin-biotinylated peroxidase complexes (Nichirei Corp., Tokyo, Japan). The peroxidase was visualized by incubation with 0.03 % 3,3′-diaminobenzidine tetrahydrochloride solution in 0.05 M Tris–HCl (pH 7.4). Sections were lightly counterstained with Mayer hematoxylin, and examined by light microscopy. Negative controls were created by using nonimmune serum or by omitting the primary antibodies.

For immunofluorescence studies, paraffin sections were incubated for 30 min in 1 % bovine serum albumin/PBS before incubation with anti-LYVE-1 antibody. Binding of the primary antibody was revealed by incubation with Rhodamine Red-X goat anti-rabbit IgG (1:100; Jackson ImmunoResearch Inc., West Grove, PA, USA). The tissue samples were mounted in ProLong Gold mounting medium and the fluorescence signals were detected with a confocal laser scanning microscope LSM 5 PASCAL (Carl Zeiss, Oberkochen, Germany).

Fig. 1 Micrographs of the lymphatics with LYVE-1 staining in the PLN of WBB6F1 mice (**a**–**f**), and analysis of PLN weight, lymphatic area fraction, lymphatic size and number both in C57BL/6J and WBB6F1 mice (**g**–**j**). CFA induces slightly increased lymphatics at early stage of the injection (Rhodamine: **a**, 2 days; **b**, 4 days; **c**, 7 days). The extended lymphatics appear in the medullary area at 4 weeks of CFA injection (**d**). After rapamycin administration, intranodal lymphatics both in shapes and numbers show little change at 2 weeks (**e**), but seem to become smaller at 4 weeks (**f**). *Co* cortex, *Me* medulla, *GC* germinal center. *Bars* 100 μm. In C57BL/6J mice, PLN weight is increased from 2 day and peaked at 7 day after CFA injection. PLN weight then becomes decreased at 2 and 4 weeks after rapamycin administration, which is inconsistent with the results of intranodal lymphatic size and area fraction ($P < 0.001$; **g**–**i**). In WBB6F1 mice, lymphatic size and area fraction in the 2-day group after CFA injection are greatly increased as compared with other groups ($P < 0.001$; **h**, **i**). The rapamycin-treated PLN shows smaller lymphatic size and area fraction at 4 weeks than at 2 weeks ($P < 0.05$; **h**, **i**). In comparison of two kinds of mice, C57BL/6J mice show much more increased intranodal lymphatic size and area fraction than WBB6F1 mice at 4–7 days and 2–4 weeks after CFA injection ($P < 0.001$; **h**, **i**). In WBB6F1 mice, the most interesting finding is a decreased number of lymphatic vessels within the first 7 days after CFA injection ($P < 0.05$; **j**)

Enzyme histochemistry

For transmission electron microscopy (TEM), PLN and skin tissues were fixed in 4 % paraformaldehyde for 3 h at 4 °C, and treated with 5′-Nase-cerium medium containing 20 mM $CeCl_3$ and 1 mM AMP for 40 min at 37 °C. After postfixed in 2 % osmium tetroxide for 2 h at 4 °C, the samples were dehydrated in a graded series of ethanol and embedded in Epon 812. Ultrathin sections (90–95 nm) were collected on 100-mesh copper grids, and stained with uranyl acetate and lead citrate. The sections were then examined with JEM-1200 EX II electron microscope (JEOL, Tokyo, Japan).

Morphometric analysis of lymphatic images

LYVE-1- and podoplanin-stained sections were photographed with a Biorevo BZ-9000 microscope (objective

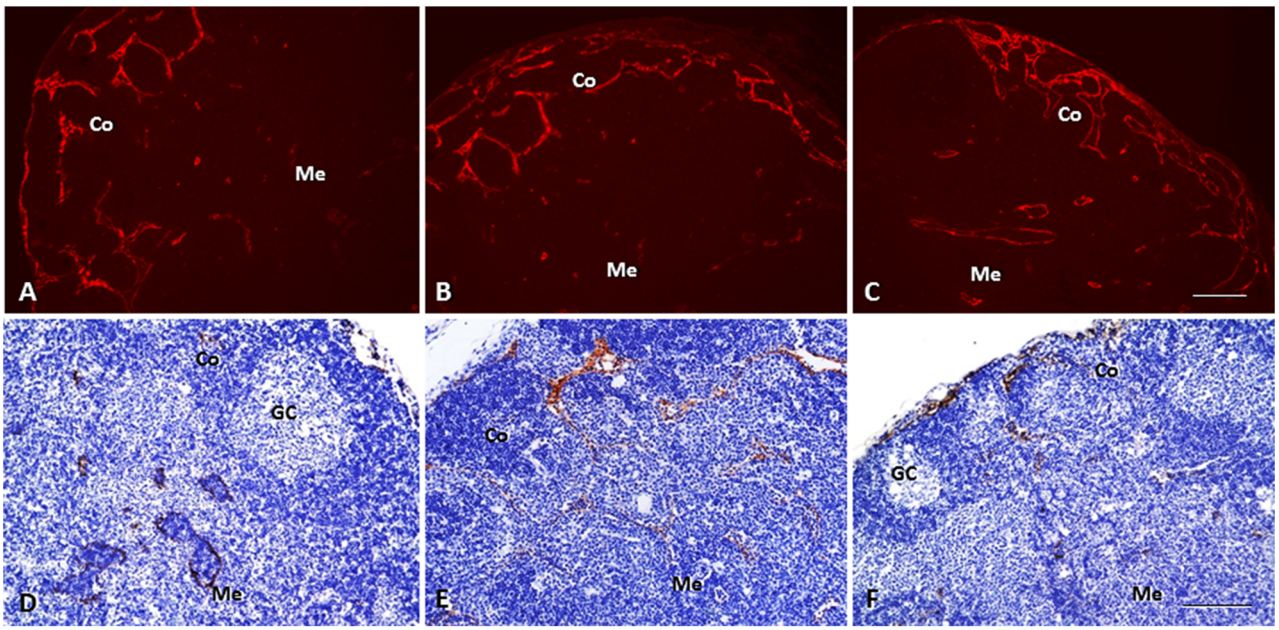
A
Co
Me
B
Co
Me
C
Co
Me
D
Co
GC
Me
E
Co
Me
F
Co
GC
Me

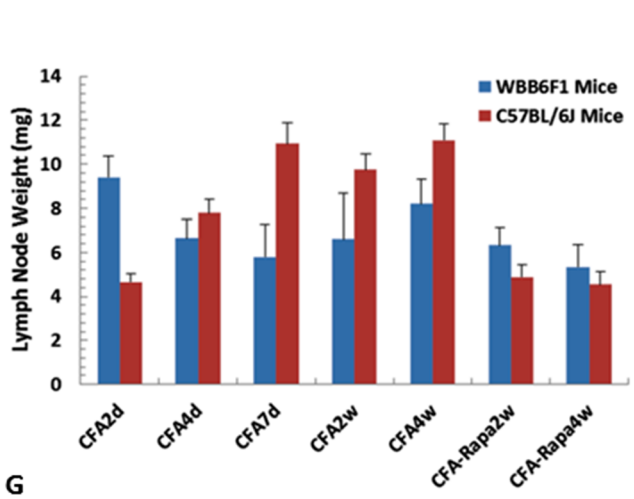
WBB6F1 Mice
C57BL/6J Mice
Lymph Node Weight (mg)
0
2
4
6
8
10
12
14
CFA2d
CFA4d
CFA7d
CFA2w
CFA4w
CFA-Rapa2w
CFA-Rapa4w
G

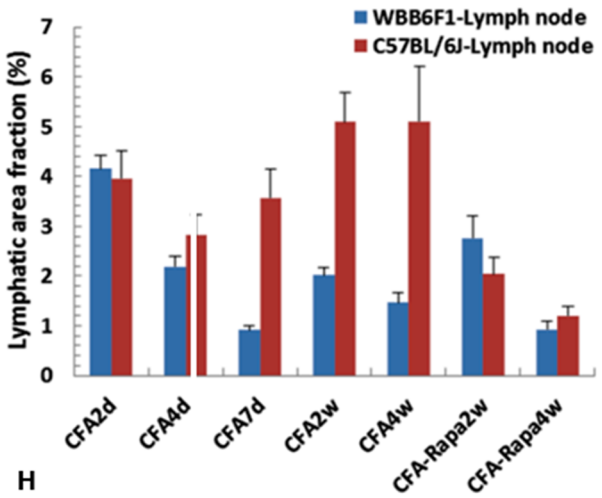
WBB6F1-Lymph node
C57BL/6J-Lymph node
Lymphatic area fraction (%)
0
1
2
3
4
5
6
7
CFA2d
CFA4d
CFA7d
CFA2w
CFA4w
CFA-Rapa2w
CFA-Rapa4w
H

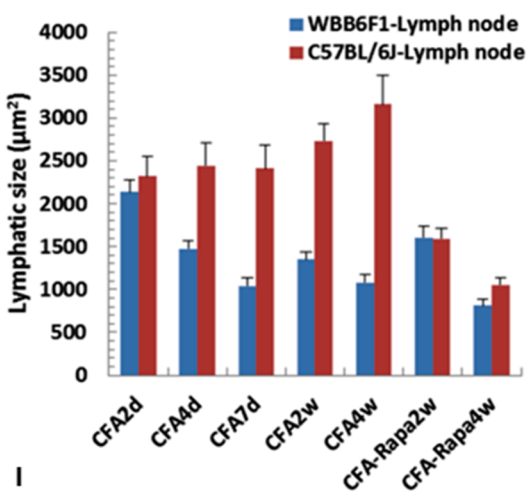
WBB6F1-Lymph node
C57BL/6J-Lymph node
Lymphatic size (μm²)
0
500
1000
1500
2000
2500
3000
3500
4000
CFA2d
CFA4d
CFA7d
CFA2w
CFA4w
CFA-Rapa2w
CFA-Rapa4w
I

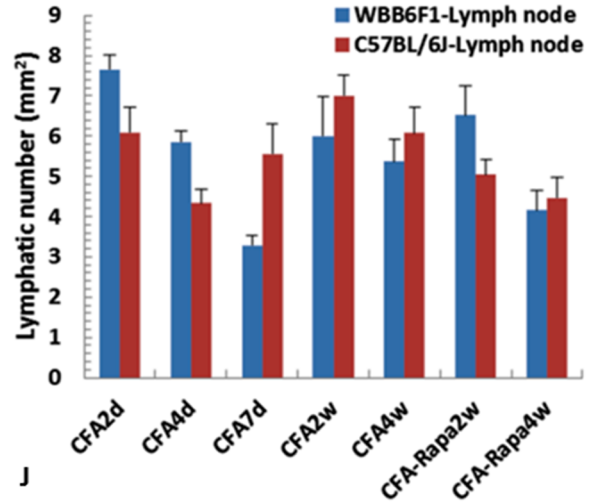
WBB6F1-Lymph node
C57BL/6J-Lymph node
Lymphatic number (mm²)
0
1
2
3
4
5
6
7
8
9
CFA2d
CFA4d
CFA7d
CFA2w
CFA4w
CFA-Rapa2w
CFA-Rapa4w
J

lens ×20, Keyence). Morphometric analyses were performed using NIH ImageJ (Version 1.47b) software to determine lymphatic vessel density (defined as the number of lymphatics per unit area, 394,024.4 μm^2), average lymphatic size, and fractional area of lymphatics (%) (the area of lymphatics per unit area of the tissue).

Reverse transcription-polymerase chain reaction (RT-PCR) analysis

The mRNA expression of VEGF-A, VEGF-C, VEGF-D, VEGFR-2, VEGFR-3, *Prox-1*, and TNF-α in the PLN and footpad skin was evaluated by semi-quantitative RT-PCR. Total RNAs were extracted using an Rneasy Mini kit (Qiagen Com. Inc., Valencia, CA, USA). First strand complementary DNA was synthesized from an RNA template (1 μg) using oligo (dT) specific sets of primers and a Qiagen one step RT-PCR kit. The RT-reaction profile was 50 °C for 30 min, followed by 95 °C for 15 min. The amplification procedure consisted of 35 cycles as follows: denaturing at 94 °C for 30 s, annealing at 57 °C for 1 min, and extending at 72 °C for 1 min and 45 s. The sequences of primers were as described previously [8, 9]. All these primers were confirmed to yield the expected products under these conditions. The specific negative control was performed by amplification of a sample containing the same reagents except reverse transcriptase. The PCR products were electrophoresed on 1.5 % agarose gels and detected by ethidium bromide staining. All RT-PCR experiments were performed in duplicate with representative images shown. The relative band intensity was quantified by using the NIH ImageJ software, and normalized to GAPDH housekeeping gene levels.

Statistical analysis

Statistical analysis was performed using Systat 11 (SYSTAT Software Inc., Point Richmond, CA, USA). For evaluation of statistical differences in the lymphatic vessel density, average size and fractional area of the skin and PLN, one-way ANOVA test followed by Bonferroni's multiple comparison tests was employed when comparing more than two groups. Values of $P < 0.05$ were considered statistically significant for each analysis.

Results

MCs may play certain role in CFA-induced intranodal lymphangiogenesis

In WBB6F1 mice, CFA injection induced early increase in PLN lymphatics, especially in the subcapsular area (Fig. 1a–d). In TEM, the subcapsular or medullary lymphatics seemed regular in contrast to C57BL/6J mice, with inflammatory cells or lymphocytes passing through the intercellular endothelial junctions (Fig. 2a–d). The response of PLN weight obviously increased at 2 days but then decreased after 7 days, and the lymphatic size and area fraction in the 2-day group were much more increased than other groups including rapamycin-treated groups ($P < 0.001$; Fig. 1g–i). Intranodal lymphatic numbers also increased at 2 and 4 days compared with 7 days ($P < 0.05$; Fig. 1j).

In CFA-stimulated C57BL/6J mice, increased and enlarged LYVE-1-positive lymphatics mainly appeared in the PLN cortex surrounding reactive germinal centers at 4 days (Fig. 3a). The lymphatics extended from the cortex to deep medulla with increased networks. During 2–4 weeks, the subcapsular and medullary lymphatics of PLN were obviously enlarged, and filled with macrophages and a large amount of lymphocytes, which were found to penetrate the endothelial wall (Fig. 3b, c; Fig. 2e–h). PLN weight was much more increased at 7 days than at 2 days ($P < 0.001$; Fig. 1g).

In comparison of two kinds of mice, C57BL/6J mice showed much more increased intranodal lymphatic size and area fraction than WBB6F1 mice, from 4 days to 4 weeks after CFA injection ($P < 0.001$; Fig. 1h, i).

Rapamycin inhibits CFA-induced intranodal lymphangiogenic response

In rapamycin-treated WBB6F1 mice, the intranodal lymphatics became scattered (Fig. 1e, f), showing smaller lymphatic size and area fraction at 4 weeks than at 2 weeks ($P < 0.05$; Fig. 1h, i).

In C57BL/6J mice, the germinal centers became smaller or less obvious in the rapamycin-treated group than in the untreated group. Lymphangiogenesis was inhibited both in the cortex and medulla where intranodal lymphatics showed a decreased tendency (Fig. 3d). PLN weight became decreased at 2 and 4 weeks, which is consistent with the results of the intranodal lymphatic size and area fraction ($P < 0.001$; Fig. 1g–i). Intranodal lymphatic numbers decreased at 4 weeks after rapamycin treatment ($P < 0.05$; Fig. 1j).

CFA-induced dermal lymphangiogenesis shows no distinction between two strains of mice

In WBB6F1 mice, the lymphatics were significantly enlarged and gathered closely in the sebaceous glands (Fig. 4a–d). The lymphatic size had a tendency becoming smaller from 4 days to 4 weeks ($P < 0.001$; Fig. 4g). The developing lymphatics showed immature features with an irregular and thicker endothelial wall, which had obvious protrusions and simple

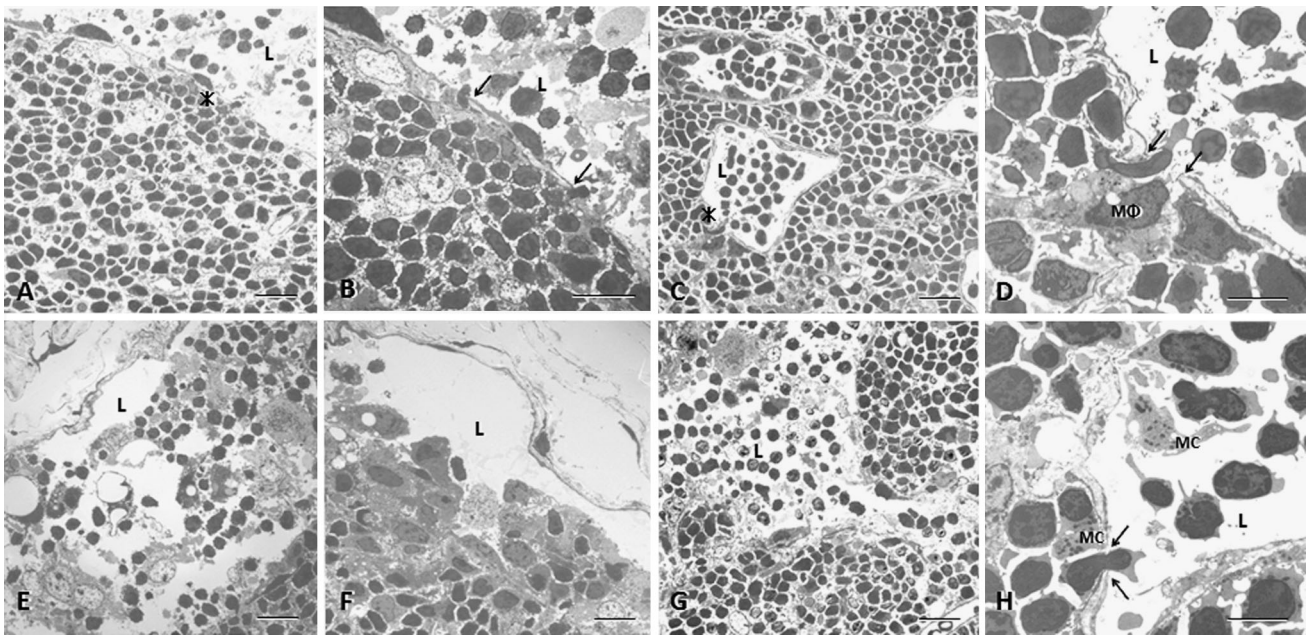

Fig. 2 TEM photographs show CFA-treated PLN lymphatics at 2 weeks. In the mast cell-deficient mice (**a**–**d**), no distinct difference is shown in the structure of subcapsular lymphatics with cell-penetration (**a**, **b**), in comparison of C57BL/6J mice. **b** shows an enlarged image of the *asterisk* in **a**. Regular medullary lymphatics show that inflammatory cells or lymphocytes pass through intercellular endothelial junctions (**c**, **d**). **d** is a high magnification image of the *asterisk* in **c**. In C57BL/6J (**e**–**h**), the distended subcapsular lymphatics contain some macrophages and a large amount of lymphocytes (**e**, **f**). The inflammatory cells or lymphocytes often penetrate the endothelial wall of enlarged medullary lymphatics (**g**, **h**). *L* lymphatic vessel, *MC* mast cell, *MΦ* macrophage, *Arrows* intercellular endothelial junctions. **a** ,**c**, **e**, **f**, **g** *Bars* 20 μm; **b** *Bar* 10 μm; **d**, **h** *Bars* 5 μm

intercellular junctions (Fig. 5a). On the contrary, the initial developed lymphatics represented a slender and irregular endothelial layer, and the mature lymphatics with subendothelial lymphocytes were decorated with 5′-Nase-cerium particles (Fig. 5b). The collecting lymphatics in the subcutaneous tissue showed typical bi-leaflet valves with 5′-Nase-cerium reaction products (Fig. 5c, d).

In CFA-stimulated C57BL/6J mice, the subdermal tissues showed numerous lymphatics with different size, and obvious infiltration of inflammatory cells at 4–7 days. These lymphatics often surrounded large blood vessels, and showed an irregular and flatten outline in the deep connective tissue (Fig. 6a–d). The lymphatic number reached the peak at 4 days, and was higher than at 7 days ($P < 0.05$; Fig. 4h), but did not show increased tendency at 2–4 weeks. CFA stimulation occasionally induced lymphangioma characterized by the lymphatic-like structure filled with inflammatory cells (Fig. 6a–d).

Rapamycin has little impact on CFA-induced dermal lymphangiogenesis

In WBB6F1 mice, the effect of rapamycin on the skin lymphatics could not be detected (Fig. 4e, f). Of interest, an increase in lymphatic size and number appeared at 2 and 4 weeks, respectively (Fig. 4g, h).

In rapamycin-treated C57BL/6J mice, the infiltration of lymphocytes was not attenuated in the subcutaneous tissue (Fig. 6e, f). Irregular changes in the lymphatic size were not influenced by CFA and rapamycin (Fig. 4g).

CFA-induced lymphangiogenesis is dependent on VEGF-A/VEGFR-2 and TNF-α both in the skin and PLN.

In CFA-treated WBB6F1 mice, the expression of VEGF-A, VEGFR-2, VEGF-D and TNF-α was markedly augmented in skin and PLN tissues, but showing no influence of rapamycin administration. In both CFA- and rapamycin-treated tissue samples, the expression of VEGF-C and VEGFR-3 was clearly detected in the PLN, but almost invisible in the skin. *Prox-1* expression in PLN was obvious in CFA-treated group, but became weak and even disappeared in rapamycin-treated group. All the skin samples treated with CFA and rapamycin showed low or no expression of *Prox-1* (Fig. 7a, b).

In CFA-treated C57BL/6J mice, PLN and skin tissues showed strong mRNA expression of VEGF-A, VEGFR-2 and TNF-α, but lacked VEGF-C, VEGFR-3 and *Prox-1* expression. With further rapamycin administration, the expression of VEGF-A, VEGFR-2 and TNF-α did not show obvious change, but the expression of VEGF-C, VEGFR-3 and *Prox-1* irregularly appeared in these tissues, especially in the PLN. VEGF-D signal was weaker in the skin than in PLN (Fig. 8a, b).

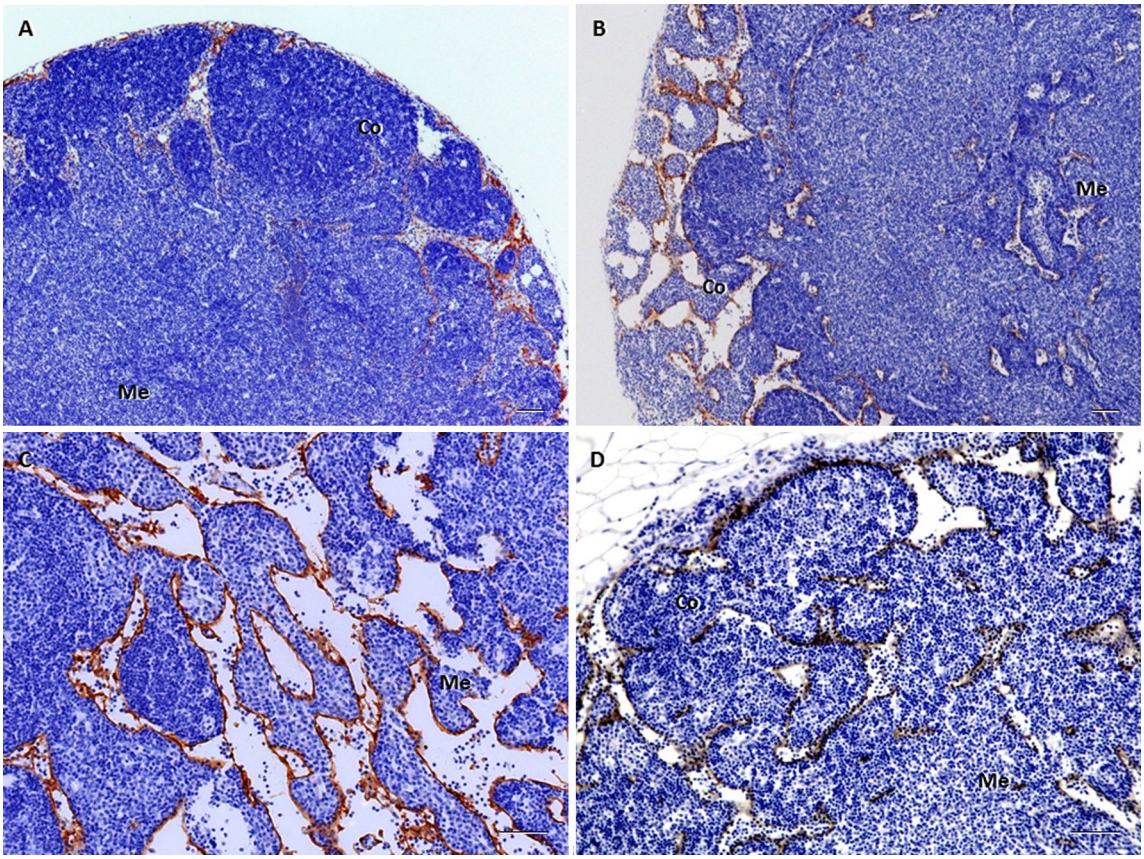

Fig. 3 Micrographs of LYVE-1-positive lymphatics in CFA-stimulated popliteal lymph nodes (PLN) of C57BL/6J mice. The increased and enlarged lymphatics mainly appear in the PLN cortex at 4 days after CFA injection (**a**). During 2–4 weeks, the lymphatics extend from the cortex to the deep medulla with increased networks, which are filled with a large amount of lymphocytes (**b**, **c**). After rapamycin treatment for 2 weeks, the lymphatics are decreased both in the cortex and medulla (**d**). *Co* cortex, *Me* medulla, *GC* germinal center. *Bars* 100 μm

Discussion

Lymphangiogenesis is known to play a causal role in several lymphatic-associated diseases. In the present study, LYVE-1-positive lymphatic analysis indicated that lymphatic size, number and area fraction increased both in the skin and PLN of CFA-treated mice. The mRNA expression of VEGF-A/VEGFR-2 and other molecules, e.g., TNF-α showed some distinctions and differences between two strains of mice, C57BL/6J and WBB6F1 mice (the MC-deficient strain). CFA-stimulated lymph node hyperplasia represented an increase in weight, but its size was not proportional to the degree of intranodal lymphangiogenesis. Intranodal lymphangiogenesis was observed mainly in the cortex but also in the medulla, indicating the reactive response may have a distinct target according to its function. During the stage, MCs may play some role in intranodal lymphangiogenesis, and rapamycin has the potential to inhibit lymphatic development of lymph nodes by intraperitoneal administration.

Lymphangiogenic factors and intranodal lymphatic hyperplasia

Lymphangiogenesis reflects a sequence of events related to endothelial cell migration, proliferation, and sprouting, as well as tubule formation and branching. The process is mediated by many molecules, including proinflammatory chemokines and cytokines, e.g., TNF-α, and growth factors [10]. The present study has showed that the expression of VEGF-A, VEGFR-2, and TNF-α is markedly augmented in the skin and PLN, indicating these factors have definite and important influences on CFA-induced lymphangiogenesis both in C57BL/6J and WBB6F1 mice. VEGF-A can trigger lymphangiogenic responses, in which B cells are required for VEGF-A expression in the immunized lymph nodes. B cells can orchestrate expansion of intranodal lymphatic networks, and lymphangiogenesis in response to CFA can be reduced by blocking its receptor, VEGFR-2 [11]. In CFA-induced inflammation, the preexisting lymphatics may become enlarged, and the newly formed lymphatics

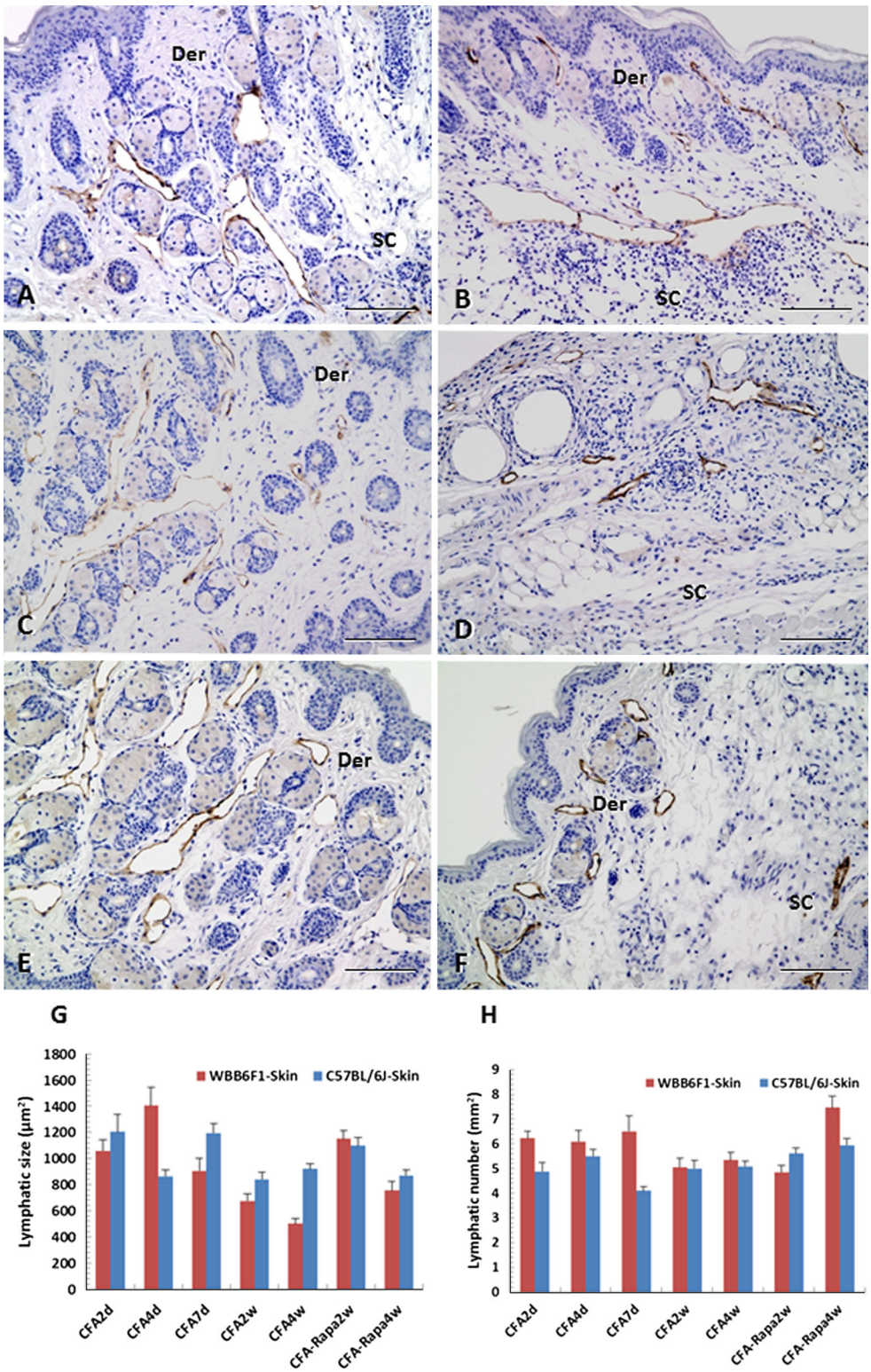

Fig. 4 The skin lymphatics with LYVE-1 staining in the dermal and subcutaneous tissues of the mast cell-deficient mice (**a**–**f**), and analysis of lymphatic size and number both in C57BL/6J and WBB6F1 mice (**g**, **h**). LYVE-1-positive lymphatics are enlarged and gathered in the sebaceous glands after CFA administration (**a** 2 days; **b** 4 days; **c** 2 weeks; **d** 4 weeks). The collecting lymphatics possess bi-leaflet valves (**b**). The lymphatic distribution and structure in the rapamycin-treated skin are similar to those of the CFA group (**e** 2 weeks; **f** 4 weeks). *Der* dermis, *SC* subcutaneous tissue. *Bars* 100 μm. In WBB6F1 mice, the dermal lymphatic size decreases from 4 days to 4 weeks after CFA injection ($P < 0.001$; **g**), but reversibly, increases after rapamycin administration ($P < 0.001$; **g**, **h**). In C57BL/6J mice, irregular changes in the dermal lymphatic size are not related with CFA and rapamycin injection (**g**). CFA-induced lymphatic number reaches the peak at 4 days ($P < 0.05$; **h**)

are intimately associated with lymphocyte infiltration and proliferation that appears well defined and nodular. Our previous studies have also indicated that expansion and high proliferation of lymphatic vessels may occur simultaneously in the acute phase of inflammation. With the modification and continuing proliferation, the lymphatic vessels may become mature and functional to adapt environmental change by regulating regional lymph

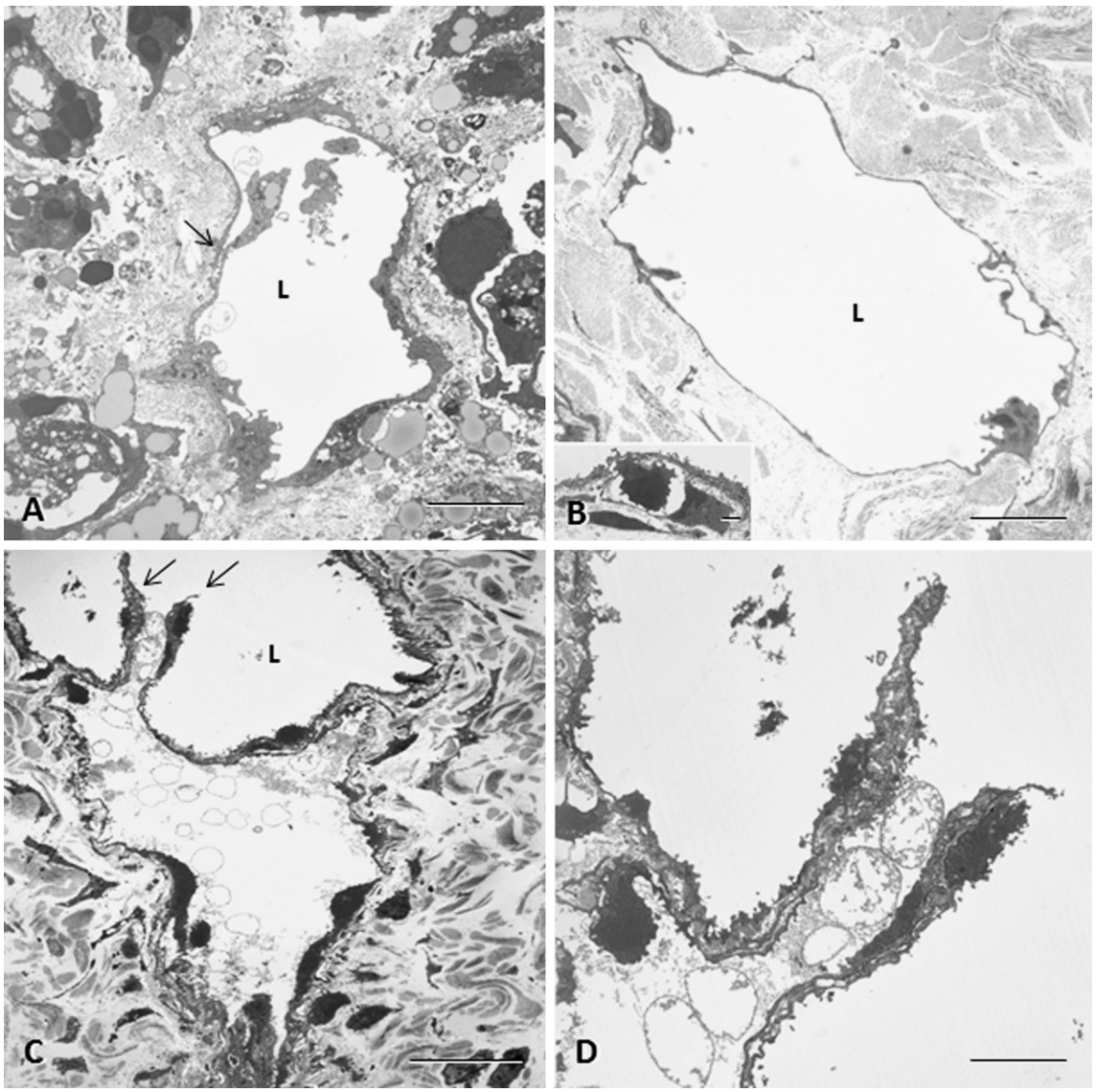

Fig. 5 TEM photographs of the dermal lymphatics in the mast cell-deficient mice without CFA or rapamycin injection. **a** The developing initial lymphatic vessel shows immature features of irregular and thicker endothelial walls. LECs have obvious protrusions and simple intercellular junctions (arrow). **b** The typical initial developed lymphatic vessel shows a slender and irregular endothelial wall. The insert picture shows the mature endothelial cells decorated with 5′-Nase-cerium particles, where a subendothelial lymphocyte can be seen. **c** The collecting lymphatic vessel in the subcutaneous tissue shows typical bi-leaflet valves (*arrows*). **d** The magnified valve apices in C are an extension structure of the lymphatic wall, labeled with 5′-Nase-cerium reaction product. *L* lymphatic vessel. **a**, **b**, **d** *Bars* 5 μm; **c** *Bar* 20 μm; *Inset Bar* 1 μm

drainage [2, 9, 10]. TNF-α, a potent mediator of inflammation through activation of NF-κB in the inflammatory cells including macrophages and lymphocytes, has been actively involved in lymphangiogenesis [2]. TNF-α can increase the transcription of VEGFR-2 gene, accounting for increased migration of endothelial cells and stimulation of wound repair triggered by VEGF-A165 [12]. TNF-α signaling inhibition impeded lymphangiogenesis in inflammation [13].

Prox-1 and VEGF-C are critical factors in developmental and pathological lymphangiogenesis. *Prox-1* is a transcription factor in the program specifying LEC fate. VEGF-C/VEGFR-3 pathway may represent a highly potent and specific target for cancer therapy. The inhibition of VEGF-C expression in tumor cells could be a potential strategy for preventing lymphatic metastasis. The present study has shown that the expression of VEGF-C, VEGFR-3 and *Prox-1* is different in the skin and PLN. In CFA-treated

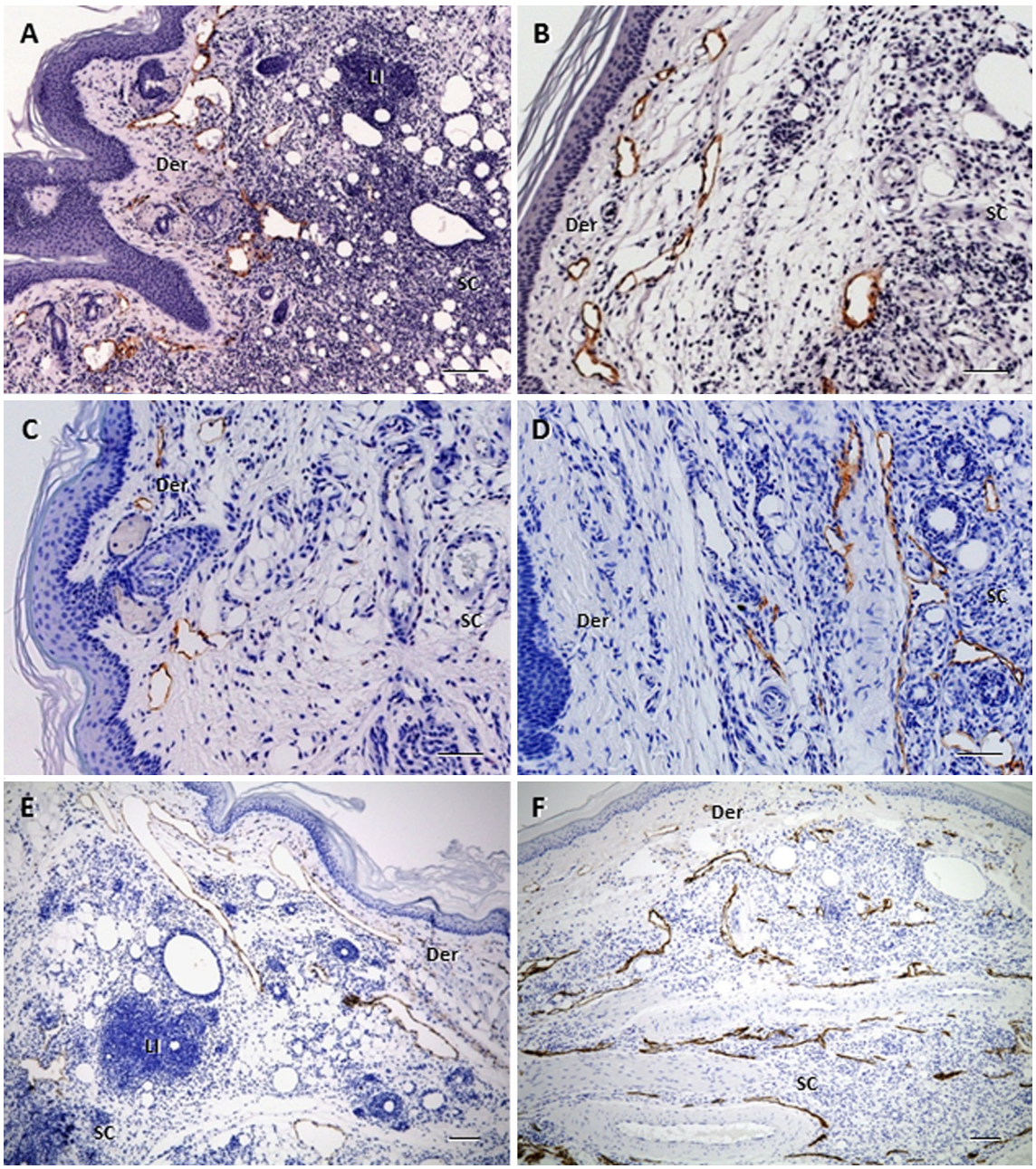

Fig. 6 The skin lymphatics with LYVE-1 staining in C57BL/6J mice. In the early stage of CFA injection, the subcutaneous tissue shows serious infiltration of inflammatory cells and numerous lymphatics with different sizes. The CFA stimulation induces lymphangiomas characterized by lymphatic-like structures filled with inflammatory cells (**a** 2 days; **b** 4 days). The lymphatics show a slight increasing tendency at 2 or 4 weeks after CFA injection. The fine lymphatics often surround blood vessels and gland ducts, showing an irregular and flattened outline in the deep connective tissue (**c** 2 weeks; **d** 4 weeks). Compared with the CFA group, the rapamycin-treated mice show little change both in LYVE-1-positive dermal lymphatic size and number (**e** 2 weeks; **f** 4 weeks). The infiltration of lymphocytes in the subcutaneous tissue is not attenuated by rapamycin administration. *Der* dermis, *SC* subcutaneous tissue, *LI* lymphocyte infiltration. *Bars* 100 μm

WBB6F1 PLN, the expression of VEGF-C, VEGFR-3 and *Prox-1* was clearly visible. With rapamycin treatment, the expression of VEGF-C/VEGFR-3 did not show any change but *Prox-1* was reduced. In CFA-stimulated C57BL/6J PLN, the expression of VEGF-C, VEGFR-3 and *Prox-1* was invisible, but shown after rapamycin administration. The expression of VEGF-C, VEGFR-3 and *Prox-1* was almost not detected in the skin of two strains of mice, indicating that these factors did not seem to respond to local CFA stimulation and rapamycin administration.

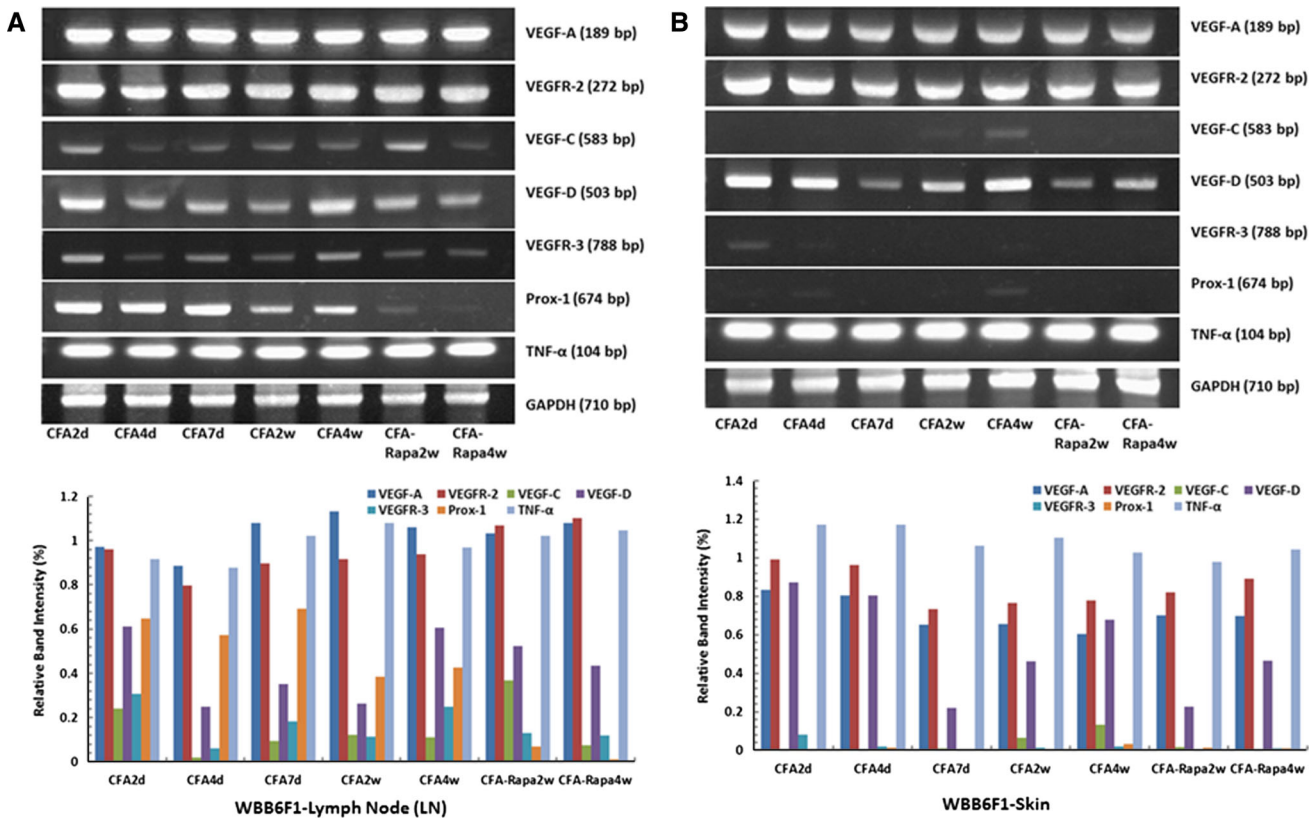

Fig. 7 RT-PCR analysis of the mRNAs for lymphangiogenic factors in the PLN (**a**) and skin (**b**) of WBB6F1 mice treated by CFA at 2,4,7 days and 2,4 weeks, and by rapamycin at 2,4 weeks. The distinct expression of mRNAs for VEGF-A, VEGF-D, VEGFR-2 and TNF-α is detected both in the skin and PLN, but the skin tissue shows little expression of VEGF-C, VEGFR-3 and *Prox-1*, in comparison with the detectable expression in PLN. Lower panels show image analysis of RT-PCR results. Intensity of individual bands is quantified using ImageJ densitometry software, and normalized to GAPDH housekeeping gene levels

VEGF-D, a member of VEGF family, can induce both angiogenesis and lymphangiogenesis by activating VEGFR-2 and VEGFR-3, leading to enhanced tumor metastasis [14, 15]. Although VEGF-D signal is slightly weaker in the skin than in PLN, it could not exclude the action of VEGF-D/VEGFR-2 axis in CFA-induced lymphangiogenesis. Clearly, the biological significance and molecular mechanisms underlying the interplay among MCs, rapamycin and CFA-induced lymphangiogenesis still remain to be determined.

MC deficiency interferes with regional lymphangiogenesis

MCs play an important role in the perpetuation of allergic responses by producing multifunctional cytokines and chemokines that recruit and activate other cells to the inflammatory and tumor microenvironment. MCs are among the first immune cells to infiltrate the tumor, contributing to human cancer progression by promoting angiogenesis [16]. In the Myc-induced pancreatic islet tumors, MCs were demonstrated to be essential for angiogenesis, and for tumor growth and sustainment [17]. High MC density may correlate with either favorable or unfavorable prognostic significance in inflammatory and tumor pathogenesis.

MC-derived mediators stored in cytoplasmic granules like cytokine TNF-α regulate the development of adaptive immunity and local inflammatory responses via interacting with the lymphatic system. Lymphatic vesicles appear to be conduits for the trafficking of discrete MC particles to lymph nodes [18]. It seems likely that MC modulation may be involved in lymphatic structure and function in response to lymphangiogenic factors. Genetically MC-deficient mutant mice have become a powerful tool for identifying and quantifying the contribution of MCs in many biological responses in vivo [19]. In CFA-treated WBB6F1 mice, increased intranodal lymphatic size and area fraction at the first 2 days may indicate an early lymphatic enlargement rather than lymphangiogenesis. Moreover, the continuing reduction in dermal lymphatic size may reflect a structural regression following lymphangiogenesis. The newly formed lymphatics are small in the superficial subcutaneous tissue, and much less in number in the deep layer. The findings have suggested that MC deficiency may involve in different tissue reactions to CFA-induced lymphangiogenesis in

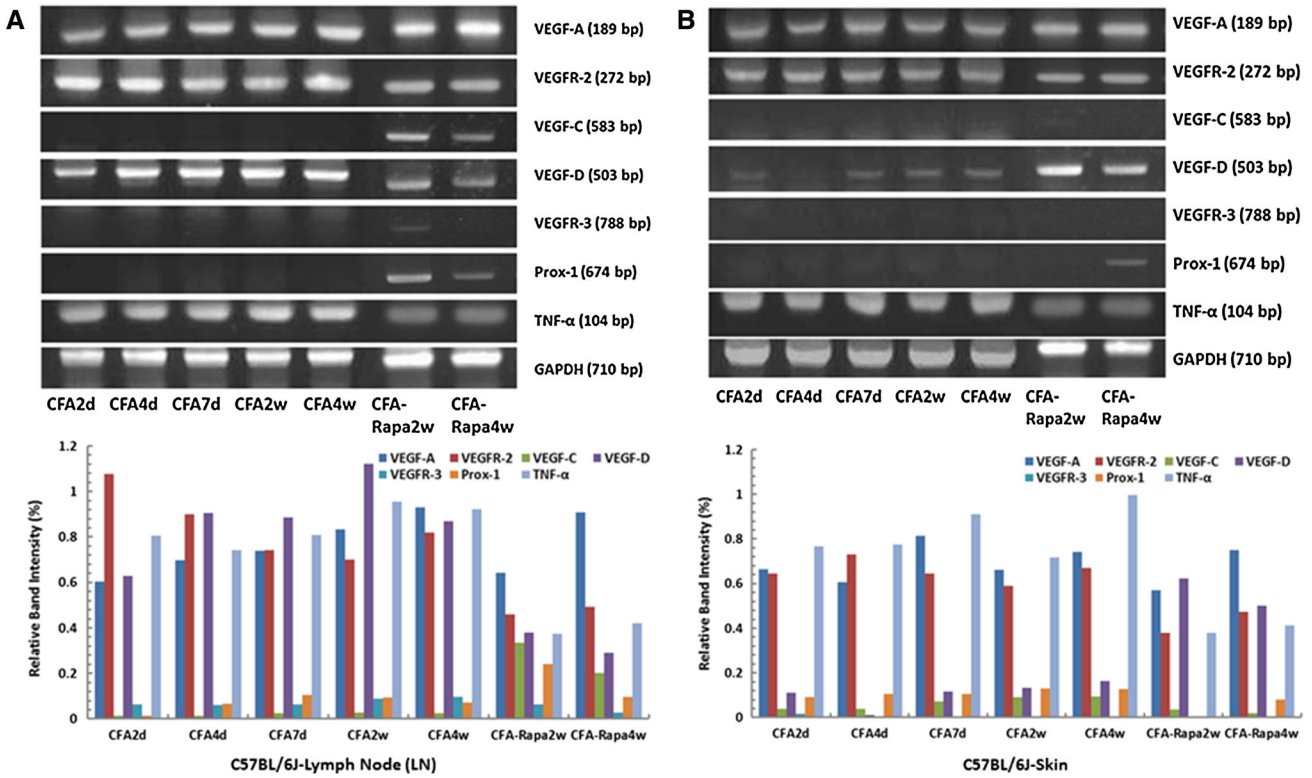

Fig. 8 RT-PCR analysis of the mRNAs for lymphangiogenic factors in the PLN (**a**) and skin (**b**) of C57BL/6J mice treated by CFA at 2,4,7 days and 2,4 weeks, and by rapamycin at 2,4 weeks. CFA-treated PLN and skin tissues show strong expression of mRNAs for VEGF-A, VEGFR-2 and TNF-α, but lack expression of VEGF-C, VEGFR-3 and *Prox-1*. VEGF-D expression is much weaker in the skin than in PLN. The expression of VEGF-A, VEGFR-2 and TNF-α is not changed due to rapamycin administration, but conversely the mRNAs of VEGF-C, VEGFR-3 and *Prox-1* are detectable in PLN, even indistinctly expressed in the skin tissue. Lower panels show image analysis of RT-PCR results. Intensity of individual bands is quantified using ImageJ densitometry software, and normalized to GAPDH housekeeping gene levels

WBB6F1 mice. Comparatively, the intranodal lymphatic response to CFA stimulation is much higher in C57BL/6J than in WBB6F1 mice, probably indicating a malfunction resulting from MC deficiency in the latter mice. Currently, the role of MC-endothelial cell axis to immune homeostasis is emphasized by the fact that some of the most effective treatments for inflammatory disorders are directed at interfering with this interaction [18]. Obviously, how MCs influence lymphangiogenesis is related to our understanding of lymphatic biology in inflammation and tumor metastasis.

Rapamycin inhibits inflammatory lymphangiogenesis in PLN

Rapamycin acts as a specific inhibitor of mTOR, a serine/threonine kinase, and appears to be downstream of the phosphoinositide-3′ kinase (PI3K)/Akt signal pathway [20]. mTOR is required for the maturation and differentiation of multiple immune cell lineages. It has been noted that rapamycin and its analogs exert a potent antitumor action on a variety of solid tumors, and have antiangiogenic properties related to the suppression of VEGF signal transduction. As a consequence, in vivo primary and metastatic tumor growth and microvessel density were strikingly reduced by rapamycin administration [21].

The anti-lymphangiogenic effect of rapamycin is one of the mechanisms responsible for suppressing tumor progression, suggesting that mTOR regulates lymphangiogenesis as well. The lymphangiogenic signal via VEGFR-3 activates the Akt-dependent pathway and promotes the proliferation of LECs [22, 23]. Inhibition of LECs by rapamycin plays an important role in the mTOR-Akt signaling pathway. Rapamycin potently interferes with the activation of LECs by inhibiting VEGF-C or downregulating VEGFR-3 protein expression, showing significant inhibition of LEC proliferation, migration and tube formation in vitro [24, 25], and impairs recovery of lymph flow in a dermal wound model [24]. In a rapamycin-treated tumor mouse model, the number of lymphatic vessels was greatly decreased and the lymph node metastasis was significantly suppressed [5]. The inhibition of mTOR with rapamycin may exert its antitumoral activity at multiple

steps, reducing growth and metastasis of primary tumors, and blocking intratumoral lymphangiogenesis without perturbing normal distribution of lymphatic vessels [6]. The present findings in two strains of mice showed that rapamycin may play a small role in CFA-induced intranodal lymphangiogenesis. However, it seems difficult to deduce that the intraperitoneal administration of rapamycin can modulate CFA-induced lymphangiogenesis in the injected footpads because of the irregular change in dermal lymphatic size and number. Simultaneously, stable TNF-α expression also suggests that rapamycin may not be involved in lymphatic regulation by proinflammatory cytokines. mTOR inhibition with rapamycin may represent a suitable therapeutic option for controlling numerous processes essential for lymphangiogenesis including cell growth, proliferation, motility, and survival in inflammation and cancers. However, a possible role of the PI3K/Akt/mTOR pathway in MC deficiency and rapamycin administration needs to be studied in the future.

References

1. Ji RC (2006) Lymphatic endothelial cells, lymphangiogenesis, and extracellular matrix. Lymphat Res Biol 4:83–100
2. Ji RC (2012) Macrophages are important mediators of either tumor- or inflammation-induced lymphangiogenesis. Cell Mol Life Sci 69:897–914
3. Ishizuka T, Terada N, Gerwins P, Hamelmann E, Oshiba A, Fanger GR, Johnson GL, Gelfand EW (1997) Mast cell tumor necrosis factor alpha production is regulated by MEK kinases. Proc Natl Acad Sci USA 94:6358–6363
4. Detoraki A, Staiano RI, Granata F, Giannattasio G, Prevete N, de Paulis A, Ribatti D, Genovese A, Triggiani M, Marone G (2009) Vascular endothelial growth factors synthesized by human lung mast cells exert angiogenic effects. J Allergy Clin Immunol 123:1142–1149
5. Kobayashi S, Kishimoto T, Kamata S, Otsuka M, Miyazaki M, Ishikura H (2007) Rapamycin, a specific inhibitor of the mammalian target of rapamycin, suppresses lymphangiogenesis and lymphatic metastasis. Cancer Sci 98:726–733
6. Patel V, Marsh CA, Dorsam RT, Mikelis CM, Masedunskas A, Amornphimoltham P, Nathan CA, Singh B, Weigert R, Molinolo AA, Gutkind JS (2011) Decreased lymphangiogenesis and lymph node metastasis by mTOR inhibition in head and neck cancer. Cancer Res 71:7103–7112
7. Lesma E, Eloisa C, Isaia E, Grande V, Ancona S, Orpianesi E, Di Giulio AM, Gorio A (2012) Development of a lymphangioleiomyomatosis model by endonasal administration of human TSC2 (−/−) smooth muscle cells in mice. Am J Pathol 181:947–960
8. Ji RC, Eshita Y, Kato S (2007) Investigation of intratumoural and peritumoural lymphatics expressed by podoplanin and LYVE-1 in the hybridoma-induced tumours. Int J Exp Pathol 88:257–270
9. Ji RC, Eshita Y, Xing L, Miura M (2010) Multiple expressions of lymphatic markers and morphological evolution of newly formed lymphatics in lymphangioma and lymph node lymphangiogenesis. Microvasc Res 80:195–201
10. Ji RC (2009) Lymph node lymphangiogenesis: a new concept for modulating tumor metastasis and inflammatory process. Histol Histopathol 24:377–384
11. Angeli V, Ginhoux F, Llodrà J, Quemeneur L, Fenette PS, Skobe M, Jessberger R, Merad M, Randolph GJ (2006) B cell-driven lymphangiogenesis in inflamed lymph nodes enhances dendritic cell mobilization. Immunity 24:203–215
12. Giraudo E, Primo L, Audero E, Gerber HP, Koolwijk P, Soker S, Klagsbrun M, Ferrara N, Bussolino F (1998) Tumor necrosis factor-alpha regulates expression of vascular endothelial growth factor receptor-2 and of its co-receptor neuropilin-1 in human vascular endothelial cells. J Biol Chem 273:22128–22135
13. Baluk P, Yao LC, Feng J, Romano T, Jung SS, Schreiter JL, Yan L, Shealy DJ, McDonald DM (2009) TNF-alpha drives remodeling of blood vessels and lymphatics in sustained airway inflammation in mice. J Clin Investig 119:2954–2964
14. McColl BK, Paavonen K, Karnezis T, Harris NC, Davydova N, Rothacker J, Nice EC, Harder KW, Roufail S, Hibbs ML, Rogers PA, Alitalo K, Stacker SA, Achen MG (2007) Proprotein convertases promote processing of VEGF-D, a critical step for binding the angiogenic receptor VEGFR-2. FASEB J 21:1088–1098
15. Karnezis T, Shayan R, Caesar C, Roufail S, Harris NC, Ardipradja K, Zhang YF, Williams SP, Farnsworth RH, Chai MG, Rupasinghe TW, Tull DL, Baldwin ME, Sloan EK, Fox SB, Achen MG, Stacker SA (2012) VEGF-D promotes tumor metastasis by regulating prostaglandins produced by the collecting lymphatic endothelium. Cancer Cell 21:181–195
16. Dalton DK, Noelle RJ (2012) The roles of mast cells in anticancer immunity. Cancer Immunol Immunother 61:1511–1520
17. Soucek L, Lawlor ER, Soto D, Shchors K, Swigart LB, Evan GI (2007) Mast cells are required for angiogenesis and macroscopic expansion of Myc-induced pancreatic islet tumors. Nat Med 13:1211–1218
18. Kunder CA, St John AL, Abraham SN (2011) Mast cell modulation of the vascular and lymphatic endothelium. Blood 118:5383–5393
19. Grimbaldeston MA, Chen CC, Piliponsky AM, Tsai M, Tam SY, Galli SJ (2005) Mast cell-deficient W-sash c-kit mutant Kit W-sh/W-sh mice as a model for investigating mast cell biology in vivo. Am J Pathol 167:835–848
20. Mèndez R, Myers MG Jr, White MF, Rhoads RE (1996) Stimulation of protein synthesis, eukaryotic translation initiation factor 4E phosphorylation, and PHAS-I phosphorylation by insulin requires insulin receptor substrate 1 and phosphatidylinositol 3-kinase. Mol Cell Biol 16:2857–2864
21. Guba M, von Breitenbuch P, Steinbauer M, Koehl G, Flegel S, Hornung M, Bruns CJ, Zuelke C, Farkas S, Anthuber M, Jauch KW, Geissler EK (2002) Rapamycin inhibits primary and metastatic tumor growth by antiangiogenesis: involvement of vascular endothelial growth factor. Nat Med 8:128–135
22. Mäkinen T, Veikkola T, Mustjoki S, Karpanen T, Catimel B, Nice EC, Wise L, Mercer A, Kowalski H, Kerjaschki D, Stacker SA, Achen MG, Alitalo K (2001) Isolated lymphatic endothelial cells transduce growth, survival and migratory signals via the VEGF-C/D receptor VEGFR-3. EMBO J 20:4762–4773
23. Salameh A, Galvagni F, Bardelli M, Bussolino F, Oliviero S (2005) Direct recruitment of CRK and GRB2 to VEGFR-3 induces proliferation, migration, and survival of endothelial cells through the activation of ERK, AKT, and JNK pathways. Blood 106:3423–3431
24. Huber S, Bruns CJ, Schmid G, Hermann PC, Conrad C, Niess H, Huss R, Graeb C, Jauch KW, Heeschen C, Guba M (2007) Inhibition of the mammalian target of rapamycin impedes lymphangiogenesis. Kidney Int 71:771–777
25. Luo Y, Liu L, Rogers D, Su W, Odaka Y, Zhou H, Chen W, Shen T, Alexander JS, Huang S (2012) Rapamycin inhibits lymphatic endothelial cell tube formation by downregulating vascular endothelial growth factor receptor 3 protein expression. Neoplasia 14:228–237